Pharmacological Reports (2022) 74:684–695
https://doi.org/10.1007/s43440-022-00379-8

ARTICLE

Synthetic lipoproteins based on apolipoprotein E coupled to fullerenol have anti-atherosclerotic properties

Irina Florina Tudorache[1] · Violeta Georgeta Bivol[1] · Madalina Dumitrescu[1] · Ioana Madalina Fenyo[1] · Maya Simionescu[1] · Anca Violeta Gafencu[1]

Received: 4 March 2022 / Revised: 4 June 2022 / Accepted: 8 June 2022 / Published online: 5 July 2022

Abstract

Background Apolipoprotein E (apoE) is an anti-atherosclerotic protein associated with almost all plasma lipoproteins. Fullerenol (Full-OH) contains the fullerene hydrophobic cage and several hydroxyl groups that could be derivatized to covalently bind various molecules. Herein, we aimed to produce fullerenol-based nanoparticles carrying apoE3 (Full-apoE) and test their anti-atherosclerotic effects.

Methods Full-apoE nanoparticles were obtained from Full-OH activated to reactive cyanide ester fullerenol derivative that was further reacted with apoE protein. To test their effect, the nanoparticles were administered to apoE-deficient mice for 24 h or 3 weeks. ApoE part of the nanoparticles was determined by Western Blot and quantified by ELISA. Atherosclerotic plaque size was evaluated after Oil Red O staining and the gene expression was determined by Real-Time PCR.

Results Full-apoE nanoparticles were detected mainly in the liver, and to a lesser extent in the kidney, lung, and brain. In the plasma of the Full-apoE-treated mice, apoE was found associated with very-low-density lipoproteins and high-density lipoproteins. Treatment for 3 weeks with Full-apoE nanoparticles decreased plasma cholesterol levels, increased the expression of apolipoprotein A-I, ABCA1 transporter, scavenger receptor-B1, and sortilin, and reduced the evolution of the atheromatous plaques in the atherosclerotic mice.

Conclusions In experimental atherosclerosis, the administration of Full-apoE nanoparticles limits the evolution of the atheromatous plaques by decreasing the plasma cholesterol level and increasing the expression of major proteins involved in lipid metabolism. Thus, they represent a novel promising strategy for atherosclerosis therapy.

Graphical abstract

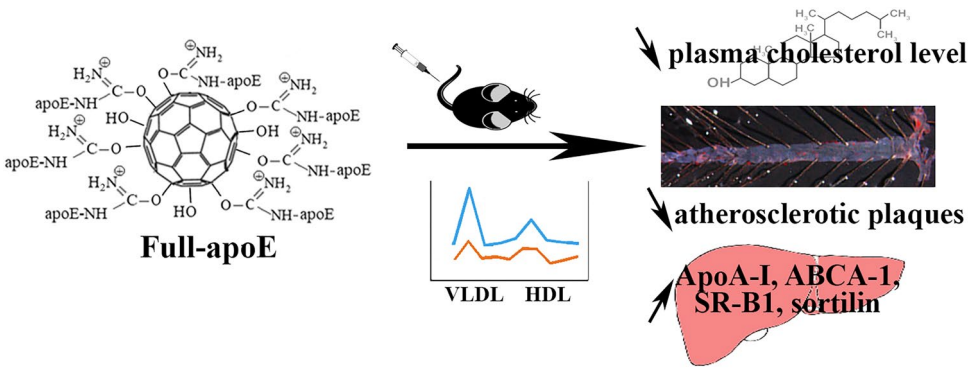

Keywords Apolipoprotein E · Atherosclerosis · Cholesterol · Nanoparticles · Fullerenol

✉ Anca Violeta Gafencu
anca.gafencu@icbp.ro

[1] Institute of Cellular Biology and Pathology "N. Simionescu", Bucharest, Romania

Abbreviations

apoE	Apolipoprotein E
cho	Cholesterol

Full-apoE	Apolipoprotein E covalently bound to Fullerenol
Full-OH	Fullerenol
HDL	High-density lipoprotein
LDL	Low-density lipoprotein
PBS	Phosphate-buffered saline
SD	Standard deviation
SEM	Standard error of the mean
VLDL	Very low-density lipoprotein

Introduction

Atherosclerosis is a multifactorial disease that may ultimately lead to major complications, such as stroke, myocardial infarction, and heart failure. The atherosclerotic lesions occur in the first decades of life and develop continuously in arterial lesion-prone areas [1]. Accumulation of plasma cholesterol, endothelial cell activation, dysfunction [2, 3], and the robust inflammatory reaction including immune cell infiltration and foam cell formation are the main events of atheroma development [4, 5]. Thus far, the anti-atherosclerotic therapy was focused mainly on either lowering plasma cholesterol levels to limit the subendothelial lipid accumulation or targeting various molecular pathways [6–8]. However, there is no efficient treatment leading to atheroma regression yet. Enhancement of the lipid efflux from the foam cells residing within the atherosclerotic plaque by various nanotechnology approaches could be a promising strategy for atheromatous plaque regression [9].

Apolipoprotein E (apoE, 35 kDa) is an anti-atherosclerotic protein that facilitates hepatic and extrahepatic uptake of lipoproteins and cholesterol efflux from foam cells [10]. Besides, apoE has anti-oxidant and anti-inflammatory properties, as reviewed in [11]. In the plasma, apoE is systemically delivered by the liver [12], while a small but important amount is produced and locally provided by macrophages [13]. As we previously reported, physiological apoE levels are maintained by complex regulatory mechanisms, that function under the influence of various circumstances, such as inflammation, stress factors, and hormones [14]. It was reported that apoE deficiency in mice leads to atherosclerosis [15]. In humans, there are three structural different apoE isoforms: apoE2, apoE3, and apoE4. Of these, apoE3 is the most common isoform, apoE2 is associated with an increased risk of heart disease and apoE4 is correlated with Alzheimer's Disease, as reviewed in [16].

Fullerene (C60) is a spherical hollow-cage molecule (~ 1 nm diameter) with carbon atoms arranged in a network of hexagons and pentagons, which belongs to the class of inorganic nanoparticles [17]. Since its discovery in 1985, it has been extensively used in various biomedical applications, such as drug and gene delivery [17]. The fullerene core is hydrophobic, but functional groups can be attached to bind proteins, DNA, or other molecules. This functionalization may allow selective tissue targeting or controlled release. Fullerene can be derivatized by hydroxylation and the obtained product, fullerenol [$C60(OH)_x$] is water soluble, thus being considered a good candidate as a drug carrier [18, 19]. Several beneficial effects of the fullerenol itself (anti-oxidant and anti-inflammatory activities) were reported, suggesting its therapeutic potential [20, 21].

We hypothesized that fullerenol-based nanoparticles carrying apoE3 (Full-apoE) could mimic apoE-rich lipoproteins and provide significant anti-atherosclerotic benefits. Here, we report that fullerenol-apoE nanoparticles administered to the $apoE^{-/-}$ atherosclerotic mice were incorporated in HDL and VLDL fractions and inhibited the evolution of the atheromatous plaques by increasing hepatic expression of the main molecules involved in lipid metabolism (apoA-I, ABCA1, SR-B1, and sortilin) and decreasing the plasma cholesterol level.

Materials and methods

Chemicals

Fullerenol (793248), potassium bromide (60093-1KG-F), cyanogen bromide solution (S261610), Oil Red O (O0625), MTT (041M6343), and EDTA (E5134) were purchased from Sigma-Aldrich (St. Louis, MO). Human recombinant apoE3 produced in a mammalian expression system (#CI02) was from Novoprotein (Millburn, NJ, USA). DMEM and fetal calf serum were from EuroClone (Milan, Italy). Tri-RNA Reagent was from Favorgen (Wien, Austria). GoTaq DNA polymerase was from Promega Corp. (Madison, WI). Primers were from Microsynth AG (Balgach, Switzerland). The high-Capacity cDNA reverse transcription kit and Sybr Green mix were from Applied Biosystems (CA, USA). Midori Green Advanced DNA Stain (MG-02) was from Nippon Genetics (Germany). The human apolipoprotein E ELISA development kit (3712-1H-20) and anti-mouse apoA-I mAb mHDL93, purified (3750-3-250) and biotinylated anti-mouse apoA-I mAb mHDL36 (3750-6-250) were from Mabtech (Germany). Cholesterol CHOD PAP and Triglycerides Kits (D95116 and D00389) were from DIALAB (Wien, Austria). Anti-human apoE was from Immuno-Biological Laboratory (IBL #18171, Gunma, Japan). Biotech Cellulose membranes with a cut-off size of 50 kDa and SuperSignal West Pico Chemiluminescence substrate were from ThermoFisher Scientific (MA, USA). RNA save (01-891-1A) was from Biological Industries (Portland, CT, USA).

Nanoparticles preparation

Full-apoE nanoparticles were obtained starting from fullerenol (Full-OH) in two steps, as illustrated in Fig. 1A. First, the hydroxyl groups of fullerenol were activated with cyanogen bromide (CNBr), leading to reactive cyanate ester groups in the fullerenol derivative (Full-CN), then Full-apoE nanoparticles were obtained by covalent binding of NH2 residues of apoE to the reactive CN groups of Full-CN (Fig. 1A). To derivatize Full-OH into cyanate ester, 1 mg fullerenol was mixed with 100 µl of 50 mM CNBr in 0.2 M borate buffer pH 8.5 (BB) and 130 µl BB for 15 min at room temperature. The stoichiometric ratio of the Full-OH: CNBr was 1:7, when the limited amount of CNBr introduced in the reaction was enough for the derivatization of seven hydroxyl groups out of the forty hydroxyl groups present on the fullerenol molecule, and the whole amount of the CNBr was used in the reaction. ApoE3 was coupled to the reactive groups of the cyanate ester fullerenol derivative in a molar ratio of Full-CN: apoE of 1:7, in 500 µl PBS, by incubation for 2 h at room temperature. The mixture was then dialyzed against PBS for 24 h at 4 °C, using a 50 kDa cut-off cellulose membrane, to remove the uncoupled protein. Then, the nanoparticles formed by apoE linked to fullerenol (Full-apoE) were sterile filtered and the bound apoE content was determined. The size of Full-OH and Full-apoE nanoparticles was determined using a Malvern Zetasizer Nano (Malvern Instruments, UK). All measurements were performed in aqueous solutions at room temperature, in triplicates.

Cell culture

HepG2 hepatocytes and EA.hy926 endothelial cells line were from ATCC. Hepatocytes were cultured in 4.5‰ glucose DMEM and endothelial cells in 1‰ glucose DMEM containing 10% fetal bovine serum (FBS) in an incubator at 37 °C, with 5% CO_2.

Assessment of cytotoxicity of Full-apoE and Full-OH nanoparticles

To test the prepared nanoparticles for possible cytotoxic effects, we employed cultured endothelial cells and hepatocytes, and we examined whether Full-apoE and Full-OH nanoparticles influence (i) the proliferation curves, measuring the cell index in time using the xCELLigence System and (ii) the cellular metabolic activity using 3-(4,5-dimethyl thiazolyl-2)-2,5-diphenyltetrazolium bromide (MTT test).

For the proliferation assay, the cells were seeded on E-plates at a density of 1×10^4 cells/well in a final volume of 100 µl and incubated at 37 °C with 5% CO_2 in the xCELLigence RTCA system. After 24 h, the Full-apoE and Full-OH nanoparticles were added at a concentration of 28 µg/ml nanoparticles (determined as apoE content or fullerenol) in

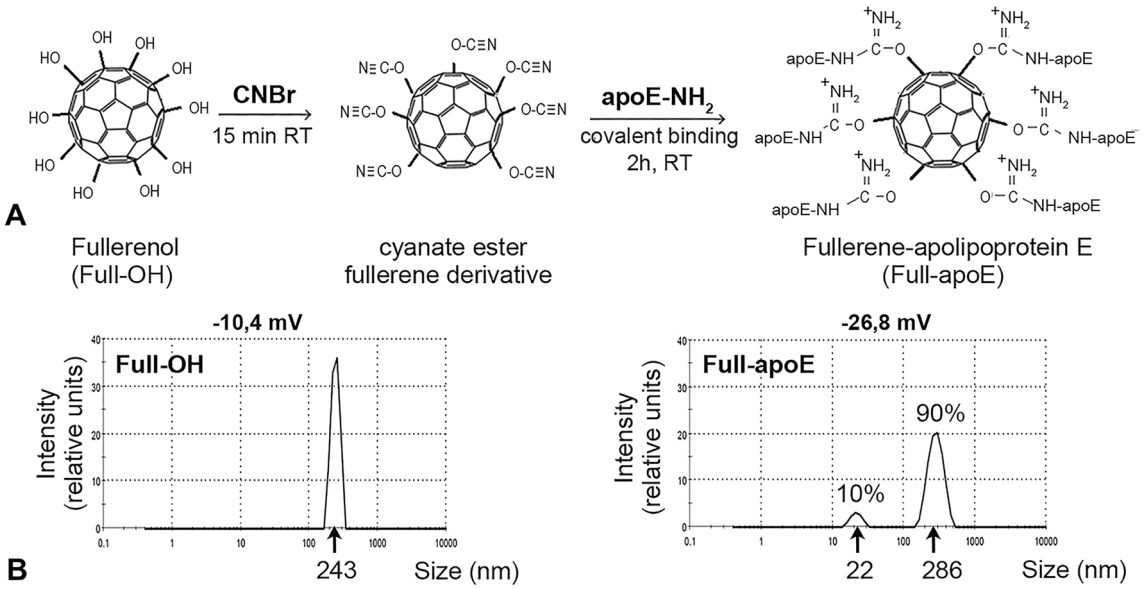

Fig. 1 Preparation and characterization of Fullerenol-apolipoprotein E nanoparticles (Full-apoE). **A** Full-apoE nanoparticles were obtained in two steps: (i) activation of a limited number of hydroxyl groups of fullerenol (Full-OH) to reactive cyanate ester groups, (ii) covalent binding of amino residues of apoE proteins to cyanate ester fullerenol derivative. **B** The size of the hydrated Full-OH nanoparticles was ~ 243 nm and of Full-apoE nanoparticles was ~ 286 nm (~ 90%) and ~ 22 nm (~ 10%). The overall surface charge of the nanoparticles was found to be negative with an absolute zeta potential value of − 10.4 mV for Full-OH nanoparticles and − 26.8 mV for Full-apoE nanoparticles

a final volume of 200 µl. In the control, the cells were incubated with 100 µl cell culture medium and 100 µl PBS. The cell proliferation was monitored on the RTCA system for 100 h. The cell index was normalized to the values obtained at 24 h when the nanoparticles were added. Each experimental condition was tested in triplicate or quadruplicate.

For the metabolic activity test, endothelial cells and hepatocytes were seeded in 96-well plates, at a density of 5×10^4 cells/well in 150 µl normal culture medium (DMEM with 10% FBS) and were incubated overnight at 37 °C and 5% CO_2. Then, the medium was replaced with 100 µl colorless medium (DMEM without phenol red containing 10% FBS), and 100 µl of Full-apoE (28 m µg/ml apoE), Full-OH (28 µg/ml) or PBS, and incubated for 18 h, at 37 °C. Afterward, the nanoparticles were removed and the cells were incubated with 150 µl colorless medium containing 0.5 mg/ml MTT. The formazan formed was solubilized in 200 µl 0.1 N HCl in isopropanol (15 min at room temperature). The absorbance of the formazan formed in the cells was measured at 570 nm, and the nonspecific background values were determined at 690 nm. The data were reported as a percentage of the control counts. All assays were performed in triplicate.

Animal experimentation

ApoE$^{-/-}$ mice were kept in SPF conditions, receiving food and water ad libitum, and exposed to 12-h light and dark cycles. Eight-week-old apoE$^{-/-}$ mice were fed with a high-fat diet (1% cholesterol, 15% butter) 1 month before the administration of the nanoparticles, as well as during the treatment. The mice were randomly distributed into three groups which were intravenously treated with: (i) Full-apoE nanoparticles, 0.6 mg apoE/kg; (ii) Full-OH nanoparticles, 0.3 mg fullerenol/kg; (iii) sterile PBS. The injections were administered in the tail vein either as (a) one single dose and the mice were sacrificed after 24 h, or as (b) one weekly dose for 3 weeks, and the mice were sacrificed at 72 h after the last injection (Fig. 2A). For both experimental conditions, the blood was collected by cardiac puncture and the organs of interest (liver, spleen, lungs, kidney, and brain) were immediately harvested. The samples were stored in

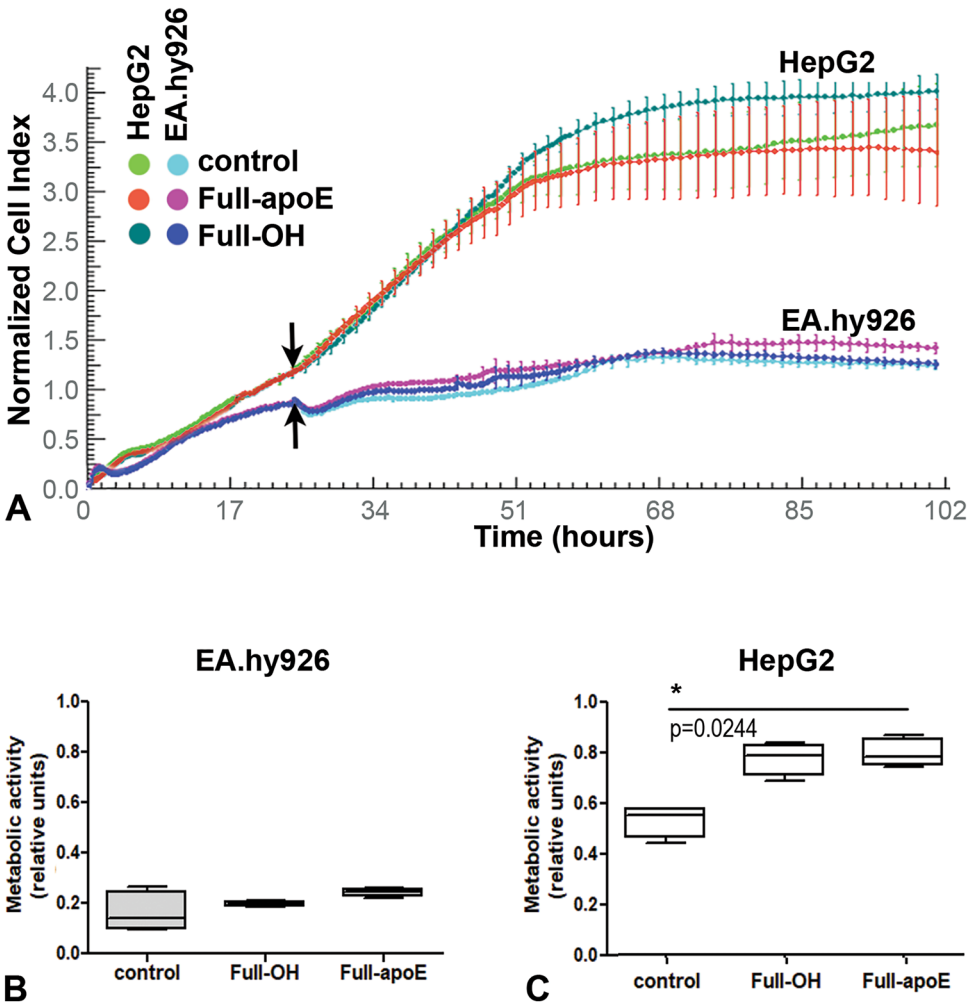

Fig. 2 Full-apoE and fullerenol nanoparticles are not cytotoxic. **A** Proliferation curves of cultured HepG2 hepatocytes and EA.hy926 endothelial cells after exposure to Full-apoE, Full-OH nanoparticles, or PBS vehicle (control) evaluated by xCELLigence RTCA system. The cell index was normalized at 24 h, the timepoint of nanoparticles addition (arrows). Data show that, for both cell lines, the nanoparticles did not interfere with cell proliferation, the differences being not statistically significant. The plots were generated by RTCA Software 1.1. and the error bars represent the SEM. **B** MTT tests revealed that Full-apoE and Full-OH nanoparticles did not affect the metabolic activity of the endothelial cells (Kruskal–Wallis test $H=4.192$, $p=0.1229$). **C** The metabolic activity of HepG2 cells was stimulated by the nanoparticles (Kruskal–Wallis and the post hoc Dunn's Multiple Comparison test $H=7.423$, $p=0.0244$). Data are represented by Whiskers plot with min and max

RNA Save for subsequent analysis or in RIPA buffer (10 mM Tris HCl pH 8, 1 mM EDTA, 1% Triton X-100, 0.1% sodium deoxycholate, 0.1% sodium dodecyl sulfate, 140 mM NaCl, 1 mM PMSF). At the end of the experiments, the aortas from the mice subjected to three weeks of treatment were harvested, fixed in PFA 4%, and stained with Oil Red O for en face evaluation of the atherosclerotic lesions using AxioVision software. For quantification of apoE within organs, the liver, lung, kidney, and the brain were milled in RIPA buffer and the supernatants collected after centrifugation (5 min at 16000*g*) were subjected to ELISA.

Determination of cholesterol and triglycerides in plasma

The blood collected on EDTA was centrifuged for 10 min at 2000×*g* to obtain the plasma. Cholesterol and triglycerides levels were determined using the corresponding kits.

Western blot

The plasma from each experimental group was pooled and an aliquot was subjected to 5–15% SDS-PAGE followed by transfer of proteins onto the nitrocellulose membrane. Blots were incubated with an anti-human apoE antibody (IBL), followed by HRP-conjugated anti-rabbit IgG and SuperSignal West Pico Chemiluminescence substrate to reveal the bands.

Lipoprotein fractions isolation

Pooled plasmas from each experimental group were fractionated using potassium bromide by density ultracentrifugation gradient (1.23 g/ml, 1.21 g/ml, 1.063 g/ml, 1.019 g/ml), at 120,000*g* for 18 h at 4 °C, using an SW55Ti rotor and a Beckman Coulter ultracentrifuge. After ultracentrifugation, fractions of 0.5 ml were collected and dialyzed against PBS.

ApoE and ApoA-I quantification by ELISA

The plates were coated with 100 µl/well of capture 2 µg/ml anti-apoE (mAb E276) or anti-apoA-I (3750-3-250), overnight at 4 °C. Then, the unspecific sites were blocked with 200 µl/well of PBS with 0.05% Tween 20 and 0.1% BSA (incubation buffer) for 1 h, at room temperature. After washing with PBS containing 0.05% Tween 20 (washing buffer), 100 µl/well of samples or standards were added and incubated for 2 h, at room temperature. Each plate was washed 5 times with washing buffer. Then, 100 µl/well of detection (1 µg/ml) biotinylated anti-apoE (mAb E887-biotin) or biotinylated anti-apoA-I (3750-6-250) were added and incubated for 1 h at room temperature. After washing, 100 µl/well of Streptavidin-HRP were added followed by incubation (1 h) at room temperature. The excess of Streptavidin-HRP was removed and the reaction was developed using TMB substrate, stopped using 0.2 M H_2SO_4, and evaluated by measuring the optical density at 450 nm.

Real-time PCR

Total RNA was extracted using Tri-RNA Reagent and revers-transcribed to complementary DNA using a High-Capacity cDNA reverse transcription kit (Applied Biosystems). The levels of apoA-I apoA-II; apoC-I, apoC-II, apoC-III, ABCA1, SR-B1, and sortilin gene expression were tested by Real-Time PCR using specific primers (shown in Table 1) and Sybr Green mix, using 7900HT Fast Real-Time PCR System with 384-Well Block (Applied Biosystems, USA). The expression of each target gene was normalized to the 18S reference gene level.

Statistics

Data distribution was analyzed using D'Agostino & Pearson omnibus normality test. Non-parametric Kruskal–Wallis tests followed by post hoc Dunn's Multiple Comparison were performed using GraphPad Prism 5 Software (San Diego, USA). Differences with $p < 0.05$ (*), were considered significant, while those with $p > 0.05$ were not significant. The results were presented in bars chart as median with range or as Whiskers (min to max).

Table 1 The sequences of the primers used in real-time PCR experiments

	Forward	Reverse
apoA-I	CAAAGACAGCGGCAGAGAC	CACCTTCTGTTTCACTTCC
ABCA1	GCTACCCACCCTACGAACAAC	TAGACCACAGAGGGCAGAAAC
SR-B1	CCGTCCCTTTCTACTTGTCTGTCTAC	CCCAGGACCAAGATGTTAGGCAG
Sortilin	ATAACACCTTCATTCGGACGG	GGGTGGTAAAGAAGATGATGTTG
18S	GAGAAACGGCTACCACATCCAAG	GAGTCCTGTATTGTTATTTTTCGTCAC

Results

Fullerenol-apoE nanoparticles are homogenous and exhibit no cytotoxicity

First, we assessed the size and zeta potential of Full-OH and Full-apoE nanoparticles obtained as illustrated in Fig. 1A. Using Malvern Zetasizer Nano l, we found that the diameter of hydrated fullerenol nanoparticles (Full-OH) was ~ 243 nm and the surface charge had an absolute zeta potential value of − 10.4 mV (Fig. 1B). After apoE coupling, the size of the majority (~ 90%) of Full-apoE nanoparticles was ~ 286 nm and a minor amount of the particles (~ 10%) had a diameter of ~ 22 nm. The overall surface charge of the Full-apoE nanoparticles was found to be negative, with an absolute zeta potential value of − 26.8 mV (Fig. 1B).

Second, we tested the cytotoxicity of Full-apoE nanoparticles on cultured HepG2 hepatocytes and EA.hy926 endothelial cells. For this purpose, we evaluated both the proliferation (by the kinetic measurement of the cell index increase using the xCELLigence RTCA system) and the viability (by an endpoint MTT assay). The results showed that Full-apoE nanoparticles (28 µg/ml apoE) and Full-OH (28 µg/ml) did not affect the proliferation of HepG2 and EA.hy 926 cells since the proliferation indexes were similar to those of the control cells, treated only with PBS, the vehicle (Fig. 2A). The metabolic activity of EA.hy926 cells, as measured by the MTT assay, was not affected by Full-apoE or Full-OH nanoparticles (Fig. 2B). However, the data showed that Full-apoE increased the metabolic activity in HepG2 cells as shown by the Kruskal–Wallis statistic with Dunn's post hoc test ($H = 7.423$, $p = 0.0244$, Fig. 2C, black columns).

ApoE$^{-/-}$ mice treated with Full-apoE nanoparticles had smaller atherosclerotic lesions and lower cholesterol levels as compared to control mice

Next, we evaluated the effect of Full-apoE nanoparticles on the progression of atherosclerotic lesions, following the experimental design illustrated in Fig. 3. Thus, apoE$^{-/-}$ mice were fed with a high-fat diet one month before treatment and during the three weeks of treatment. The experimental groups received either (i) Full-apoE nanoparticles, 0.6 mg apoE/kg; or (ii) Full-OH nanoparticles, 0.3 mg fullerenol/kg; or (iii) PBS (the vehicle) in the control mice. As illustrated in Fig. 3A, three doses were administered weekly and, after 72 h from the last administration, mice were sacrificed, and the aortas were harvested and analyzed for lipid accumulation by Oil Red O staining. Illustrative examples of the aorta of each experimental group are presented in Fig. 3B, and all the samples are illustrated in Fig. 1 Supplemental. When we examined the atheroma plaques from the aortic arch, we detected significantly smaller lesions in the mice treated with Full-apoE nanoparticles ($n = 4$), as compared with the control (PBS-treated mice, $n = 5$) and mice that received Full-OH nanoparticles ($n = 4$), as determined by Kruskal–Wallis test ($H = 7.101$ and $p = 0.0287$) followed by Dunn's Multiple Comparison Test. However, no statistically significant differences were observed between the size of the atheromatous plaques in the thoracic aorta of the mice treated with the Full-apoE or Full-OH as compared with the control (Fig. 3D).

Measurement of the total cholesterol in mice treated with nanoparticles revealed that cholesterol levels in mice treated for 3 weeks with Full-apoE were significantly reduced, as analyzed by the Kruskal–Wallis test and Dunn's Multiple Comparison Test post hoc analysis ($H = 7.423$, $p = 0.0244$, $n = 4$) and illustrated in Fig. 4. The median value of cholesterol in the group of mice treated with Full-apoE nanoparticles was 372.6 mg/dl, significantly reduced as compared to the control group which had a median level of cholesterol of 562.5 mg/dl. Interestingly, the total cholesterol level was also slightly decreased (but not statistically significant) to a median value of 384.6 mg/dl in mice treated with Full-OH nanoparticles.

To determine whether the Full-apoE and Full-OH nanoparticles are able to decrease the cholesterol concentration shortly after treatment, a single dose of the nanoparticles was administered to apoE$^{-/-}$ mice and after 24 h the plasma was harvested and analyzed. No differences were registered in the cholesterol levels of mice treated with nanoparticles for 24 h (Fig. 4B).

The values for plasma triglycerides of Full-apoE and Full-OH-treated mice were similar to the levels of the control groups, both for long or short-time treatments (data not shown).

We also investigated the association of synthetic lipoprotein with various plasma and lipoprotein fractions. For this, pools of plasma were collected from mice treated for 24 h with a single dose of Full-apoE nanoparticles and from mice at 72 h after the third weekly injection.

In the plasma of the mice treated with Full-apoE for 24 h, we quantified 0.8 µg/ml apoE. To determine whether a higher molecular weight apoE (derived from Full-apoE nanoparticles) occurs in the plasma after in vivo administration, plasma proteins were separated on SDS-PAGE. The results showed that at the short-time treatment (24 h) plasma apoE was present as a multimer with a molecular weight higher than 180 kDa on Western Blot (Fig. 5A, plasma). The recombinant apoE (35 kDa) employed for nanoparticle preparation was used as a positive control

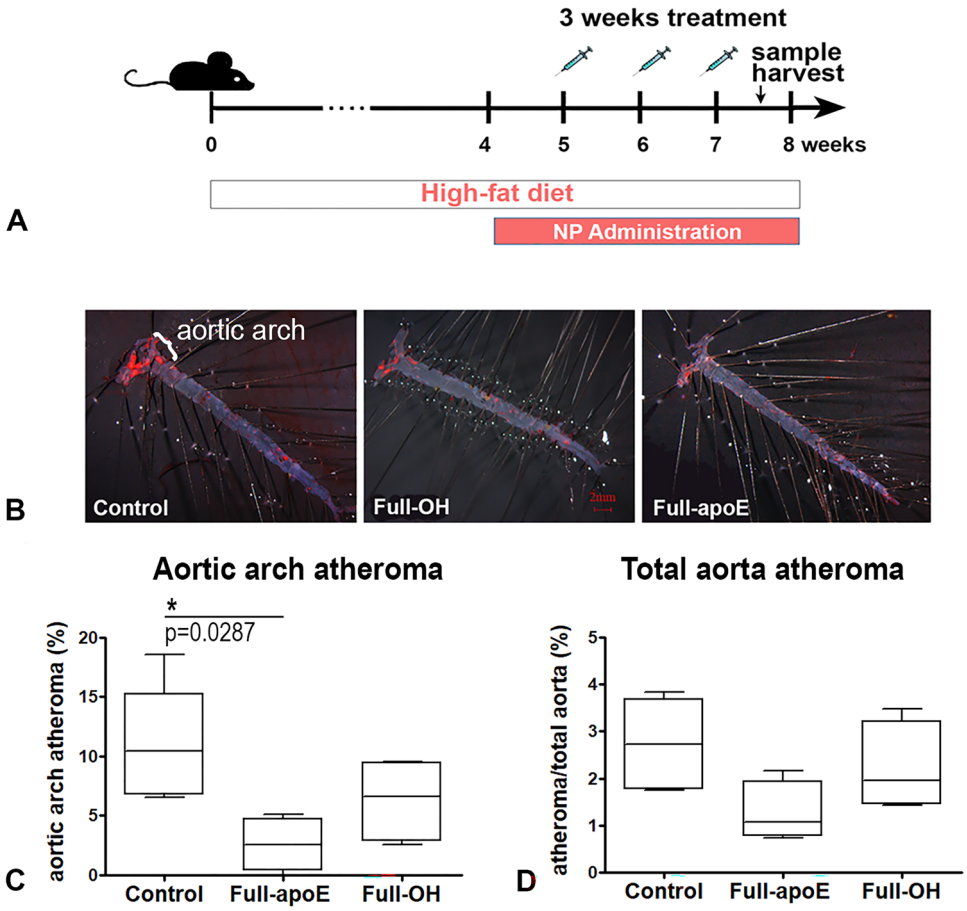

Fig. 3 The effect of Full-apoE nanoparticles on the extension of atherosclerotic plaques in apoE$^{-/-}$ mice. **A** Experimental design. ApoE$^{-/-}$ mice were fed a high-fat diet for one month before the treatment and during the interval of nanoparticles administration (one weekly dose, for 3 weeks). **B** Representative images of aortas harvested from the three animal groups: Control ($n=4$), Full-OH-treated group ($n=5$), and Full-apoE-treated group ($n=5$). Quantification of the atheromatous plaques from the aortic arch is shown in **C**, and from the whole aorta is shown in **D**. As compared with the control, the area of the lesions of mice treated with Full-apoE was significantly smaller in the aortic arch (Kruskal–Wallis statistic test with post hoc Dunn's Multiple Comparison: $H=7.101$, $p=0.0287$), tendened to decrease when reported to the total aorta ($H=5.476$, $p=0.0647$). By contrast, the size of the aortic lesions of the Full-OH-treated mice was similar to that of the control mice for all the aortic regions analyzed. Data are represented by Whiskers plot with min and max

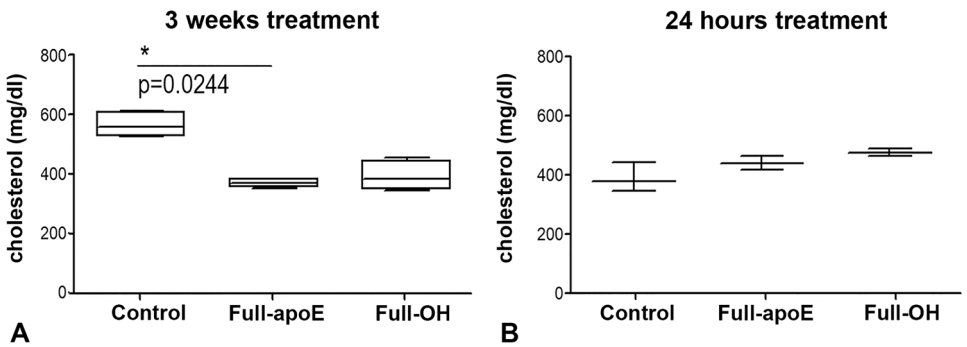

Fig. 4 Total cholesterol levels in apoE$^{-/-}$ mice treated with Full-apoE and Full-OH nanoparticles. **A** After 3 weeks of treatment, total cholesterol levels were significantly decreased in apoE$^{-/-}$ mice that received Full-apoE and Full-OH nanoparticles as compared to the control group (Kruskal–Wallis $H=7.423$ and $p=0.0244$). **B** Total cholesterol levels were not changed in apoE$^{-/-}$ mice treated with Full-apoE and Full-OH nanoparticles for 24 h treatment (Kruskal–Wallis $H=4.464$ and $p=0.1076$). Data are represented by Whiskers plot with min and max

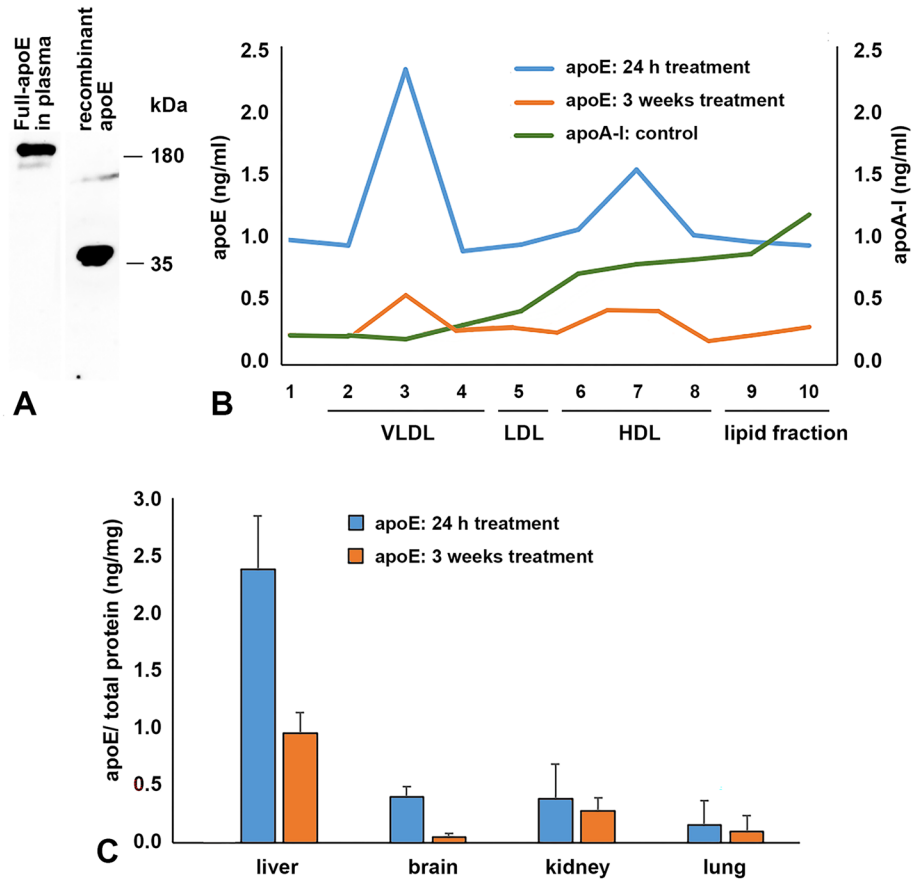

Fig. 5 Biodistribution of Full-apoE nanoparticles in plasma lipoprotein fractions and various organs of the treated mice. **A** In the plasma of mice treated with Full-apoE for 24 h, apoE was present at a higher molecular weight than (lane plasma) the monomer of the recombinant apoE (lane rec. apoE), as detected by Western Blot using an anti-apoE antibody (IBL). **B** In the lipoprotein fractions, Full-apoE nanoparticles were associated with VLDL and HDL sub-fractions at 24 h (blue line), as well as after 3 weeks of treatment (orange line). ApoA-I protein detected in the lipoprotein fraction (green line) marked the HDL fraction. **C** Full-apoE nanoparticles were present mainly in the liver and smaller amounts in the brain, kidney, and lungs at 24 h (blue columns; $n=3$) or after 3 weeks of treatment (orange columns; $n=6$). The results are shown as the mean with SD

for the specificity of the antibody (Fig. 5A, rec. apoE). No bands were obtained for apoE in the plasma of Full-OH-treated mice (data not shown). To determine the plasma distribution of apoE, pools of plasma were subjected to ultracentrifugation on the KBr gradient and 10 fractions of 0.5 ml were collected. On the gradient, the HDL fraction was identified using the apoA-I profile of the lipoprotein fraction (Fig. 5B, green line).

Both at short and long-time treatment, Full-apoE were found associated with both plasma VLDL and HDL fractions. However, a difference was detected in the ratio between the quantity in the two lipoprotein fractions. Thus, after 24 h of Full-apoE treatment, the plasma apoE was distributed mainly in the VLDL fraction and to a lesser amount in the HDL fraction (Fig. 5B, blue line), as the area under the curve for VLDL is 3.233 and for HDL is 2.572 (calculated using GraphPad Prism). At 72 h after the third weekly injection (long treatment), plasma apoE was distributed mainly in HDL and to a lesser extent in VLDL fractions, as the area under the curve for VLDL is 0.8115 and for HDL is 1.075 (Fig. 5B, orange line). Next, the biodistribution of Full-apoE nanoparticles in various organs (liver, brain, kidney, and lungs) after 24 h or 3 weeks of treatment with Full-apoE was evaluated by ELISA. In both cases, the majority of the nanoparticles were absorbed in the liver, and fewer amounts were found in the kidney and the lungs; surprisingly, Full-apoE was detected in the brain (Fig. 5B).

Hepatic apolipoproteins and receptors profile in apoE$^{-/-}$ mice treated with Full-OH and Full-apoE nanoparticles

Considering the accumulation of Full-apoE detected in the liver, we next questioned whether the hepatic expression of apolipoproteins and other molecules that interact with lipids was affected by the administration of nanoparticles in mice. Real-Time PCR data indicated that the liver expression of apoA-I (Fig. 6A), ABCA1 (Fig. 6B), SR-B1 (Fig. 6C), and sortilin (Fig. 6D) was significantly increased in the Full-apoE group ($n=5$) as compared to the control mice ($n=4$). Kruskal–Wallis test and Dunn's Multiple Comparison Test post hoc analysis revealed the statistical significance for the molecules analyzed ($p=0.0239$, $H=7.471$ for apoA-I; $p=0.0267$, $H=7.243$ for ABCA1; $p=0.0049$, $H=10.65$ for SR-B1; $p=0.0295$, $H=7.046$ for sortilin). Full-OH nanoparticles ($n=5$) did not affect the liver expression of the above-mentioned molecules (Fig. 6).

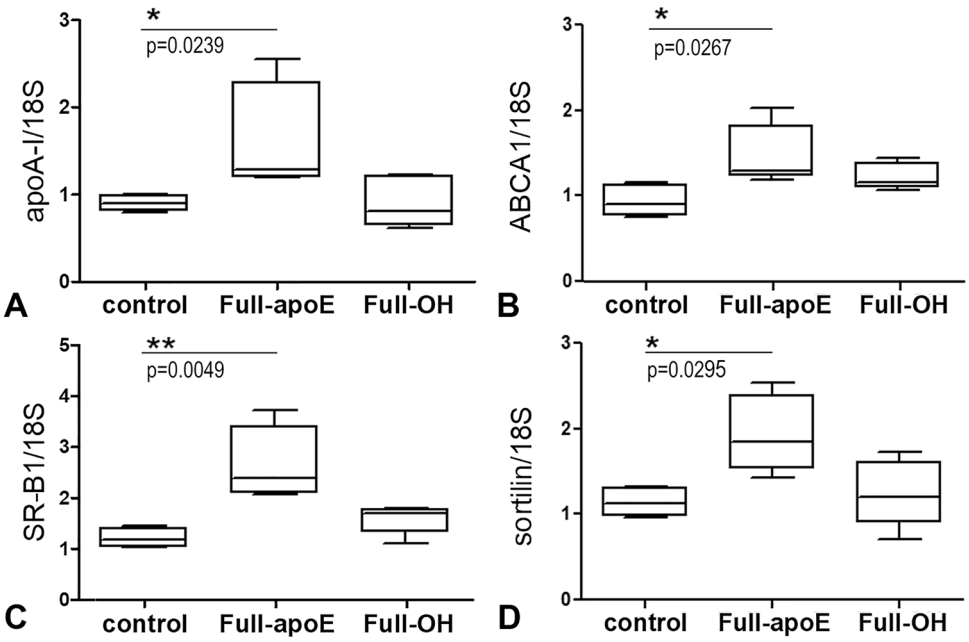

Fig. 6 Hepatic expression of apolipoprotein A-I, ABCA1, SR-B1, and sortilin in apoE$^{-/-}$ mice treated for three weeks with Full-apoE or Full-OH nanoparticles. The expression levels of apoA-I, ABCA1, SR-B1, and sortilin in the liver of the treated mice were analyzed by Real-Time PCR. Since the data have not a normal distribution, the data were statistically analyzed by Kruskal–Wallis test with Dunn's Multiple Comparison post-hoc test. Full-apoE nanoparticles significantly increased apoA-I ($H=7.471$, $p=0.0239$), ABCA1 ($H=7.243$, $p=0.0267$), SR-B1 ($H=10.65$, $p=0.0049$), and sortilin ($H=7.046$, $p=0.0295$) in the liver of treated mice, as compared with the control mice. The expression level of the analyzed molecule was not modified in the liver of Full-OH-treated mice, as compared to the control mice. Data are represented by Whiskers plot with min and max

Discussion

Apolipoprotein E is an anti-atherosclerotic protein associated with almost all types of plasma lipoproteins, able to promote de novo biosynthesis of HDL [22]. However, the presence of apoE2 isoform in humans represents a risk factor for the development of atheromatous lesions due to its low affinity for the LDL receptor.

Due to the inflammatory stress, the low amount of locally secreted apoE in the atherosclerotic plaque reduces the cholesterol efflux from the atheroma [23]. APOE knockout gene in the mouse model leads to atherogenesis [15], a pathological event counterbalanced using different strategies such as bone marrow transplantation [24, 25], adenoviral transduction [26, 27], and intramuscular injection of a plasmid encoding apoE3 [28]. Elegant studies of transgenesis showed that the sub-physiological levels of apoE in the plasma inhibited neointima formation in apoE$^{-/-}$ mice, after arterial injury [29].

In the current work, to combine the anti-atherosclerotic effects of apoE with those of fullerenol, we generated Full-apoE nanoparticles and tested whether they can reduce the atherosclerotic plaques in mice. These nanoparticles mimic apoE-rich lipoproteins, being composed of an internal hydrophobic cage that provides support to the external hydrophilic protein coat formed by apoE, both components having lipid affinity. The large majority of the nanoparticles obtained (90%) had ~ 286 nm in diameter (Fig. 1), a figure that is in the range of the size of plasma lipoproteins and is less than that of chylomicrons which may attain ~ 1200 nm in diameter [30].

To test a possible cytotoxic effect in vitro we used endothelial cells (the first cellular barrier) and hepatocytes because we considered that the liver can be the organ in which the nanoparticles would be accumulated in vivo. First, a dose–response curve of apoE nanoparticles on the cell viability was performed using 7, 14, and 28 µg apoE/ml apoE (xCELLigence experiments and MTT tests). Since the viability remained unaffected for all the doses (data not shown), here we presented the viability data using the highest dose of 28 µg apoE/ml (Fig. 2), which represents also the minimal apoE concentration in human plasma [31]. Viability data ensured that the nanoparticles would not induce deleterious effects when they would be used in vivo.

Normal plasma apoE concentration both in humans and mice is in the range of 3–10 mg/dl [32, 33]. Data from the literature showed that ectopic expression and secretion of sub-physiological levels of apoE have beneficial effects on atherosclerotic lesions. For example, very little serum apoE concentration (0.6 ng/ml) secreted in mice injected

intra-rectus femoris muscles did not affect the plasma cholesterol level, but contributed to a redistribution of cholesterol between the lipoprotein fractions, increasing the cholesterol content of HDL and decreasing it in VLDL and LDL [24]. Moreover, gene dosage experiments using transgenic mice expressing apoE in the adrenal glands demonstrated that 0.1% of the apoE levels found in normal mice decreased the plasma cholesterol by ~ 50%, being sixfold above normal [29]. When apoE reached 2–3% of the normal level, plasma cholesterol was even more reduced (being twofold above normal), preventing the foam-cells formation within the media and intima [29]. Our data showed that 24 h after Full-apoE injection, the concentration of plasma lipoprotein was ~ 0.8 ng/ml and was distributed preponderantly in the VLDL fraction and to a lesser extent in the HDL fraction. After long-time treatment apoE was distributed also in VLDL and HDL fractions, but an increased apoE-HDL/apoE-VLDL ratio was detected (from 0.8 to 1.3 for long treatment).

There were no significant differences in the weight of mice treated with Full-apoE or Full-OH compared to the control group. These results suggest that the positive effects observed in the treated mice were due to the anti-atherosclerotic potential of the nanoparticles rather than the effect of the reduced food intake due to the fat-rich diet of the mouse.

Our data demonstrated that the atherosclerotic mice treated for three weeks with Full-apoE nanoparticles (0.6 mg apoE/kg) had smaller atheromatous plaques in the aortic arch than the control mice (Fig. 3). Moreover, a reduction in the total cholesterol level was also observed in mice after the three weeks of Full-apoE administration, as compared with control mice (Fig. 4A). To highlight the possible role of the fullerenol core of Full-apoE, 0.3 mg/kg Full-OH nanoparticles were administered in apoE-deficient mice. Despite that the dose of Full-OH used was higher than that contained in the Full-apoE nanoparticles, the evolution of the atheromatous plaque was not stopped (Fig. 3). The cholesterol level of the mice treated with Full-OH nanoparticles was slightly decreased, but not statistically significant when compared to the values obtained for the control mice (Fig. 4A). This small effect may be cumulative with the apoE anti-atherosclerotic effect, and thus, one can assume that the anti-atherosclerotic effect of Full-apoE nanoparticles is due to the apoE protein, but also to the fullerenol core. This assumption is in line and extends published data that shows that fullerenol suppresses intracellular lipid accumulation, and plays an anti-oxidant role, decreasing the intracellular superoxide anion radicals [34].

ApoE from the nanoparticles was detected in various organs (liver, kidney, and lung) a distribution similar to that reported for fullerenol [35]. In the liver, mice treatment with Full-apoE or Full-OH did not change the hepatic expression levels of some inflammatory markers such as IL-2, IL-6, or TNFα (data not shown), indicating that the nanoparticles had no cytotoxic or inflammatory effects on the liver. Interestingly, even though uncoupled fullerenol was not found in the brain [35], in our experiments, Full-apoE nanoparticles crossed the blood–brain barrier (BBB) most probably by receptor-media-ted transcytosis (Fig. 5C). The affinity of apoE for the LDL receptor present in the cells of the BBB could guide the transport of nanoparticles across the BBB via the low-density lipoprotein receptor-mediated pathway [36]. The results extend the recently reported data from the literature, showing that apoE coupled to nanoparticles could increase the brain bioavailability of these drug carriers [37, 38]. Importantly, it remains to be tested whether when linked together with apoE on the activated fullerenol, the same mechanism could deliver other molecules of interest to the brain. Thus, it is safe to consider that Full-apoE nanoparticles may represent also a strategic tool for brain delivery of various drugs and molecules.

In Full-apoE-treated mice, the highest apoE concentration was found in the liver (~ 2.5 ng apoE/mg protein). As a result, we next searched for the modulation of the hepatic expression of other molecules involved in lipid metabolism. In mice treated with Full-apoE nanoparticles, we detected the upregulation of the hepatic expression of apoA-I, ABCA1, SR-B1, and sortilin (Fig. 6). These results indicated that besides its direct role, apoE may play an indirect role, modulating the expression of other major actors of the lipid metabolism—molecules involved in the synthesis of HDL (apoA-I, ABCA1, and SR-B1), as well as sortilin, which is another apoE receptor involved in the fast clearance of LDL from circulation [39]. It was reported that apoA-I induces the secretion of apoE [40] but there is no previous evidence about the effect of apoE on apoA-I. It was reported that apoE associated with apolipoprotein B-containing lipoproteins induced the upregulation of ABCA1 expression in macrophages in vitro [41]. Although we did not test this in our experimental set-up, this effect may have contributed to the atherosclerotic plaque regression observed in Full-apoE-treated mice. Thus, taken together, the upregulation of ABCA1 could improve the cholesterol efflux by apoA-I and the upregulated SR-BI mediated the cholesterol efflux by apoE.

All these properties of the Full-apoE nanoparticles showed that they represent an effective tool for atherosclerosis inhibition, even when very low apoE levels are attained. Moreover, our system may be extended in the future using mimetic apoE peptides able to mediate hepatic clearance of atherogenic lipoproteins or to combine apoE with other peptides or drugs.

Conclusions

The fullerenol-based nanoparticles carrying apoE3 mimic the apoE-rich lipoproteins providing significant anti-atherosclerotic benefits by contributing to the decrease in plasma cholesterol, and the increase in hepatic expression of apoA-I, ABCA1, SR-B1, and sortilin. The fullerenol-based nanoparticles carrying apoE3 could represent a promising novel strategy for the therapy of atherosclerosis and other inflammatory diseases.

Supplementary Information The online version contains supplementary material available at https://doi.org/10.1007/s43440-022-00379-8.

Acknowledgements We thank Mrs. Mihaela Bratu for the technical support.

Author contributions Conceptualization and data curation AVG; investigation and formal analysis, IFT, VGT, MD, and IMF; funding acquisition and project administration AVG; resources, MS; writing—original draft, IFT; writing—review and editing, VGT, MS, IMF, and AVG. All authors have read and agreed to the published version of the manuscript.

Funding This research was funded by UEFISCDI—Romania, Grant numbers PN-II-RU-TE-2014-4-2143, PN-III-P2-2.1-PED-2019-4574, and by the Romanian Academy.

Data availability The datasets generated during and/or analyzed during the current study are available from the corresponding author on reasonable request.

Declarations

Conflict of interest The authors declare no conflict of interest. The funders had no role in the design of the study; in the collection, analyses, or interpretation of data; in the writing of the manuscript, or in the decision to publish the results.

Institutional review board statement The animal experimentation was conducted following the EU Directive 63/2010 and national rules and regulations, and the protocols were approved by the Ethical Committee at the Institute of Cellular Biology and Pathology "Nicolae Simionescu" (Decision 13/13.07.2016) and National Sanitary Veterinary and Food Safety Authority—ANSVSA (authorization no. 497/2020).

References

1. Tirziu D, Dobrian A, Tasca C, Simionescu M, Simionescu N. Intimal thickenings of human aorta contain modified reassembled lipoproteins. Atherosclerosis. 1995;112(1):101–14.
2. Ghinea N, Leabu M, Hasu M, Muresan V, Colceag J, Simionescu N. Prelesional events in atherogenesis. Changes induced by hypercholesterolemia in the cell surface chemistry of arterial endothelium and blood monocytes, in rabbit. J Submicrosc Cytol. 1987;19(2):209–27.
3. Simionescu N, Mora R, Vasile E, Lupu F, Filip DA, Simionescu M. Prelesional modifications of the vessel wall in hyperlipidemic atherogenesis. Extracellular accumulation of modified and reassembled lipoproteins. Ann N Y Acad Sci. 1990;598:1–16.
4. Fenyo IM, Gafencu AV. The involvement of the monocytes/macrophages in chronic inflammation associated with atherosclerosis. Immunobiology. 2013;218(11):1376–84.
5. Manduteanu I, Simionescu M. Inflammation in atherosclerosis: a cause or a result of vascular disorders? J Cell Mol Med. 2012;16(9):1978–90.
6. Jamkhande PG, Chandak PG, Dhawale SC, Barde SR, Tidke PS, Sakhare RS. Therapeutic approaches to drug targets in atherosclerosis. Saudi Pharm J. 2014;22(3):179–90.
7. Trusca VG, Fuior EV, Gafencu AV. Beyond lipoprotein receptors: learning from receptor knockouts mouse models about new targets for reduction of the atherosclerotic plaque. Curr Mol Med. 2015;15(10):905–31.
8. Fuior EV, Trusca VG, Roman C, Gafencu AV. Enzymatic targets in atherosclerosis. J Mol Genet Med. 2015;9(3):20.
9. Calin M, Manduteanu I. Emerging nanocarriers-based approaches to diagnose and red uce vascular inflammation in atherosclerosis. Curr Med Chem. 2017;24(6):550–67.
10. Getz GS, Reardon CA. Apoprotein E and reverse cholesterol transport. Int J Mol Sci. 2018;19(11):3479.
11. Tudorache IF, Trusca VG, Gafencu AV. Apolipoprotein E—a multifunctional protein with implications in various pathologies as a result of its structural features. Comput Struct Biotechnol J. 2017;15:359–65.
12. Tangirala RK, Pratico D, FitzGerald GA, Chun S, Tsukamoto K, Maugeais C, et al. Reduction of isoprostanes and regression of advanced atherosclerosis by apolipoprotein E. J Biol Chem. 2001;276(1):261–6.
13. Bellosta S, Mahley RW, Sanan DA, Murata J, Newland DL, Taylor JM, et al. Macrophage-specific expression of human apolipoprotein E reduces atherosclerosis in hypercholesterolemic apolipoprotein E-null mice. J Clin Investig. 1995;96(5):2170–9.
14. Kardassis D, Gafencu A, Zannis VI, Davalos A. Regulation of HDL genes: transcriptional, posttranscriptional, and posttranslational. Handb Exp Pharmacol. 2015;224:113–79.
15. Zhang SH, Reddick RL, Piedrahita JA, Maeda N. Spontaneous hypercholesterolemia and arterial lesions in mice lacking apolipoprotein E. Science. 1992;258(5081):468–71.
16. Mahley RW. Apolipoprotein E: from cardiovascular disease to neurodegenerative disorders. J Mol Med (Berl). 2016;94(7):739–46.
17. Bakry R, Vallant RM, Najam-ul-Haq M, Rainer M, Szabo Z, Huck CW, et al. Medicinal applications of fullerenes. Int J Nanomed. 2007;2(4):639–49.
18. Xu B, Yuan L, Hu Y, Xu Z, Qin JJ, Cheng XD. Synthesis, characterization, cellular uptake, and in vitro anticancer activity of fullerenol-doxorubicin conjugates. Front Pharmacol. 2020;11:598155.
19. Thotakura N, Sharma G, Singh B, Kumar V, Raza K. Aspartic acid derivatized hydroxylated fullerenes as drug delivery vehicles for docetaxel: an explorative study. Artif Cells Nanomed Biotechnol. 2018;46(8):1763–72.
20. Grebowski J, Kazmierska-Grebowska P, Cichon N, Piotrowski P, Litwinienko G. The effect of fullerenol C60(OH)36 on the antioxidant defense system in erythrocytes. Int J Mol Sci. 2021;23(1):119.
21. Schuhmann MK, Fluri F. Effects of fullerenols on mouse brain microvascular endothelial cells. Int J Mol Sci. 2017;18(8):1783.
22. Zannis VI, Fotakis P, Koukos G, Kardassis D, Ehnholm C, Jauhiainen M, et al. HDL biogenesis, remodeling, and catabolism. Handb Exp Pharmacol. 2015;224:53–111.
23. Gafencu AV, Robciuc MR, Fuior E, Zannis VI, Kardassis D, Simionescu M. Inflammatory signaling pathways regulating ApoE gene expression in macrophages. J Biol Chem. 2007;282(30):21776–85.

24. Van Eck M, Herijgers N, Yates J, Pearce NJ, Hoogerbrugge PM, Groot PH, et al. Bone marrow transplantation in apolipoprotein E-deficient mice. Effect of ApoE gene dosage on serum lipid concentrations, (beta)VLDL catabolism, and atherosclerosis. Arterioscler Thromb Vasc Biol. 1997;17(11):3117–26.
25. Hasty AH, Linton MF, Swift LL, Fazio S. Determination of the lower threshold of apolipoprotein E resulting in remnant lipoprotein clearance. J Lipid Res. 1999;40(8):1529–38.
26. van Dijk KW, van Vlijmen BJ, van't Hof HB, van der Zee A, Santamarina-Fojo S, van Berkel TJ, et al. In LDL receptor-deficient mice, catabolism of remnant lipoproteins requires a high level of apoE but is inhibited by excess apoE. J Lipid Res. 1999;40(2):336–44.
27. Gerritsen G, Kypreos KE, van der Zee A, Teusink B, Zannis VI, Havekes LM, et al. Hyperlipidemia in APOE2 transgenic mice is ameliorated by a truncated apoE variant lacking the C-terminal domain. J Lipid Res. 2003;44(2):408–14.
28. Rinaldi M, Catapano AL, Parrella P, Ciafre SA, Signori E, Seripa D, et al. Treatment of severe hypercholesterolemia in apolipoprotein E-deficient mice by intramuscular injection of plasmid DNA. Gene Ther. 2000;7(21):1795–801.
29. Wientgen H, Thorngate FE, Omerhodzic S, Rolnitzky L, Fallon JT, Williams DL, et al. Subphysiologic apolipoprotein E (ApoE) plasma levels inhibit neointimal formation after arterial injury in ApoE-deficient mice. Arterioscler Thromb Vasc Biol. 2004;24(8):1460–5.
30. Zannis VI, Kypreos KE, Chroni A, Kardassis D, Zanni EE. Lipoproteins and atherogenesis. Mol Mech Atheroscler. 2004;8:111–74.
31. Han S, Xu Y, Gao M, Wang Y, Wang J, Liu Y, et al. Serum apolipoprotein E concentration and polymorphism influence serum lipid levels in Chinese Shandong Han population. Medicine (Baltimore). 2016;95(50): e5639.
32. Haddy N, De Bacquer D, Chemaly MM, Maurice M, Ehnholm C, Evans A, et al. The importance of plasma apolipoprotein E concentration in addition to its common polymorphism on inter-individual variation in lipid levels: results from Apo Europe. Eur J Hum Genet. 2002;10(12):841–50.
33. Hedrick CC, Castellani LW, Warden CH, Puppione DL, Lusis AJ. Influence of mouse apolipoprotein A-II on plasma lipoproteins in transgenic mice. J Biol Chem. 1993;268(27):20676–82.
34. Saitoh Y, Mizuno H, Xiao L, Hyoudou S, Kokubo K, Miwa N. Polyhydroxylated fullerene C(6)(0)(OH)(4)(4) suppresses intracellular lipid accumulation together with repression of intracellular superoxide anion radicals and subsequent PPARgamma2 expression during spontaneous differentiation of OP9 preadipocytes into adipocytes. Mol Cell Biochem. 2012;366(1–2):191–200.
35. Song H, Luo S, Wei H, Song H, Yang Y, Zhao W. In vivo biological behavior of 99mTc(CO)3 labeled fullerol. J Radioanal Nucl Chem. 2010;285(3):635–9.
36. Re F, Cambianica I, Zona C, Sesana S, Gregori M, Rigolio R, et al. Functionalization of liposomes with ApoE-derived peptides at different density affects cellular uptake and drug transport across a blood-brain barrier model. Nanomedicine. 2011;7(5):551–9.
37. Dal Magro R, Ornaghi F, Cambianica I, Beretta S, Re F, Musicanti C, et al. ApoE-modified solid lipid nanoparticles: a feasible strategy to cross the blood-brain barrier. J Control Release. 2017;249:103–10.
38. Bana L, Minniti S, Salvati E, Sesana S, Zambelli V, Cagnotto A, et al. Liposomes bi-functionalized with phosphatidic acid and an ApoE-derived peptide affect Abeta aggregation features and cross the blood–brain-barrier: implications for therapy of Alzheimer disease. Nanomedicine. 2014;10(7):1583–90.
39. Strong A, Ding Q, Edmondson AC, Millar JS, Sachs KV, Li X, et al. Hepatic sortilin regulates both apolipoprotein B secretion and LDL catabolism. J Clin Investig. 2012;122(8):2807–16.
40. Kockx M, Rye KA, Gaus K, Quinn CM, Wright J, Sloane T, et al. Apolipoprotein A-I-stimulated apolipoprotein E secretion from human macrophages is independent of cholesterol efflux. J Biol Chem. 2004;279(25):25966–77.
41. Zhao Y, Chen X, Yang H, Zhou L, Okoro EU, Guo Z. A novel function of apolipoprotein E: upregulation of ATP-binding cassette transporter A1 expression. PLoS One. 2011;6(7): e21453.